REPORT DOCUMENTATION PAGE	Form Approved OMB No. 0704-0188

1. REPORT DATE *(DD-MM-YYYY)*	2. REPORT TYPE	3. DATES COVERED *(From - To)*
14-01-2010	Conference Proceeding	

4. TITLE AND SUBTITLE
Polarization Characteristics of Coastal Waters and Their Impact on In-Water Visibility

5a. CONTRACT NUMBER

5b. GRANT NUMBER

5c. PROGRAM ELEMENT NUMBER
0602782N

6. AUTHOR(S)
J. Zhou, A. Tonizzo, A. Gilerson, M.S. Twardowski, Deric Gray, A. Weidemann, R. Arnone, B. Gross, F. Moshary, S. Ahmed

5d. PROJECT NUMBER

5e. TASK NUMBER

5f. WORK UNIT NUMBER
73-6369-09-5

7. PERFORMING ORGANIZATION NAME(S) AND ADDRESS(ES)
Naval Research Laboratory
Oceanography Division
Stennis Space Center, MS 39529-5004

8. PERFORMING ORGANIZATION REPORT NUMBER
NRL/PP/7330-09-9132

9. SPONSORING/MONITORING AGENCY NAME(S) AND ADDRESS(ES)
Office of Naval Research
800 N. Quincy St.
Arlington, VA 22217-5660

10. SPONSOR/MONITOR'S ACRONYM(S)
ONR

11. SPONSOR/MONITOR'S REPORT NUMBER(S)

12. DISTRIBUTION/AVAILABILITY STATEMENT
Approved for public release, distribution is unlimited.

20100121305

13. SUPPLEMENTARY NOTES

14. ABSTRACT
Polarization characteristics of coastal waters were recently measured during a cruise on the R/V "Connecticut" in the areas of New York Harbor - Sandy Hook, NJ region using a new Stokes vector instrument developed by the Optical Remote Sensing Laboratory at CCNY. The instrument has three hyperspectral Satlantic radiance sensors each with a polarizer positioned in front of it, with polarization axes aligned at 0, 90 and 45°. The measured degrees of polarization (DOPs) and normalized radiances as a function of angle and wavelength match very well with simulated ones obtained with a Monte Carlo radiative transfer code for the atmosphere-ocean system. In order to numerically reproduce the polarized images for underwater horizontal imaging system the measured typical underwater polarized radiance was used to estimate the polarized components of the background veiling light and the blurring effects were modeled by point spread functions obtained from the measured volume scattering functions from this cruise and other typical oceanic environments. It is shown that the visibility can be improved for unpolarized target by placing a polarizer oriented orthogonally to the partially polarized direction of the veiling light before camera. The blurring effects strongly depend on the small angle scattering in the forward directions. For polarized targets the Monte Carlo simulation of slab geometry for polarized pencil light shows that the scattering medium with high g value has a very strong ability to retain the polarization status of the incident light, which can be utilized to improve the image contrasts for targets with very different polarized reflection properties.

15. SUBJECT TERMS
polarization, volume scattering function, visibility

16. SECURITY CLASSIFICATION OF: a. REPORT	b. ABSTRACT	c. THIS PAGE	17. LIMITATION OF ABSTRACT	18. NUMBER OF PAGES	19a. NAME OF RESPONSIBLE PERSON
Unclassified	Unclassified	Unclassified	UL	8	Deric Gray
					19b. TELEPHONE NUMBER *(Include area code)* 228-688-4237

PUBLICATION OR PRESENTATION RELEASE REQUEST

Pubkey: 6113 NRLINST 5600.2

1. REFERENCES AND ENCLOSURES	2. TYPE OF PUBLICATION OR PRESENTATION		3. ADMINISTRATIVE INFORMATION
Ref: (a) NRL Instruction 5600.2 (b) NRL Instruction 5510.40D Encl: (1) Two copies of subject paper (or abstract)	( ) Abstract only, published ( ) Book ( ) Conference Proceedings (refereed) ( ) Invited speaker ( ) Journal article (refereed) ( ) Oral Presentation, published ( ) Other, explain	( ) Abstract only, not published ( ) Book chapter (X) Conference Proceedings (not refereed) ( ) Multimedia report ( ) Journal article (not refereed) ( ) Oral Presentation, not published	STRN NRL/PP/7330-09-9132 Route Sheet No. 7330/ Job Order No. 73-6369-09-5 Classification X U C Sponsor ONR BASE approval obtained ___ yes X no

4. AUTHOR

Title of Paper or Presentation

Polarization Characteristics of Coastal Waters and Their Impact on In-Water Visibility

Author(s) Name(s) (*First,MI,Last), Code, Affiliation if not NRL*

J. Zhou, A. Tonizzo, A. Gilerson, M.S. Twardowski, Deric Gray, Alan D. Weidemann, Robert A Arnone, B. Gross, F. Moshary, S. Ahmed

It is intended to offer this paper to the SPIE Defense, Security and Sensing 2009 Symposium
(Name of Conference)

13-APR - 17-APR-09, Orlando, FL, Unclassified
(Date, Place and Classification of Conference)

and/or for publication in SPIE Defense, Security and Sensing 2009 Symposiu
(Name and Classification of Publication) *(Name of Publisher)*

After presentation or publication, pertinent publication/presentation data will be entered in the publications data base, in accordance with reference (a).
It is the opinion of the author that the subject paper (is ____) (is not X) classified, in accordance with reference (b).
This paper does not violate any disclosure of trade secrets or suggestions of outside individuals or concerns which have been communicated to the Laboratory in confidence. This paper (does ____) (does not X) contain any militarily critical technology.
This subject paper (has ____) (has never X) been incorporated in an official NRL Report.

Deric Gray, 7334
Name and Code *(Principal Author)* (Signature)

5. ROUTING/APPROVAL

CODE	SIGNATURE	DATE	COMMENTS
Author(s) Gray		3/23	Need by 10 Apr 09 Publicly accessible sources used for this publication
Section Head Weidemann	Alan D. Weidemann	3/23/09	Looks Good!
Branch Head Robert A Arnone, 7330	William J Teague	3/23	
Division Head Ruth H. Preller, 7300		3/23	1. Release of this paper is approved. 2. To the best knowledge of this Division, the subject matter of this paper (has ____) (has never X) been classified.
Security, Code 1226			1. Paper or abstract was released. 2. A copy is filed in this office. 55099-9
Office of Counsel,Code 1008.3			
ADOR/Director NCST E. R. Franchi, 7000			
Public Affairs *(Unclassified/ Unlimited Only)*, Code 7030.4	Carolyn L Gilion	4/13/09	
Division, Code			
Author, Code			

HQ-NRL 5511/6 (Rev. 12-98) (e) THIS FORM CANCELS AND SUPERSEDES ALL PREVIOUS VERSIONS

9-1226-1220

PUBLICATION OR PRESENTATION RELEASE REQUEST

Pubkey: 6113 NRLINST 5600.2

Ref: (a) NRL Instruction 5600.2
(b) NRL Instruction 5510.40D

Encl: (1) Two copies of subject paper (or abstract)

( ) Abstract only, published
( ) Book
( ) Conference Proceedings (refereed)
( ) Invited speaker
( ) Journal article (refereed)
( ) Oral Presentation, published
( ) Other, explain

( ) Abstract only, not published
( ) Book chapter
(X) Conference Proceedings (not refereed)
( ) Multimedia report
( ) Journal article (not refereed)
( ) Oral Presentation, not published

STRN NRL/PP/7330-09-9132
Route Sheet No. 7330/
Job Order No. 73-6369-09-5
Classification X U ___ C
Sponsor ONR BASE
approval obtained ___ yes X no

Title of Paper or Presentation
Polarization Characteristics of Coastal Waters and Their Impact on In-Water Visibility

Author(s) Name(s) (First,MI,Last), Code, Affiliation if not NRL

J. Zhou, A. Tonizzo, A. Gilerson, M.S. Twardowski, Deric Gray, Alan D. Weidemann, Robert A Arnone, B. Gross, F. Moshary, S. Ahmed

It is intended to offer this paper to the SPIE Defense, Security and Sensing 2009 Symposium
(Name of Conference)

13-APR - 17-APR-09, Orlando, FL, Unclassified
(Date, Place and Classification of Conference)

and/or for publication in SPIE Defense, Security and Sensing 2009 Symposiu
(Name and Classification of Publication) (Name of Publisher)

After presentation or publication, pertinent publication/presentation data will be entered in the publications data base, in accordance with reference (a).
It is the opinion of the author that the subject paper (is ____) (is not X) classified, in accordance with reference (b).
This paper does not violate any disclosure of trade secrets or suggestions of outside individuals or concerns which have been communicated to the Laboratory in confidence. This paper (does ____) (does not X) contain any militarily critical technology.
This subject paper (has ____) (has never X) been incorporated in an official NRL Report.

Deric Gray, 7334
Name and Code (Principal Author) (Signature)

CODE	SIGNATURE	DATE	COMMENTS
Author(s) Gray	[signature]	3/23/09	Need by 10 Apr 09
			This is a Final Security Review. Any changes made in the document after approved by Code 1226 nullify the Security Review
Section Head Weidemann	[signature]	3/23/09	looks good!
Branch Head Robert A Arnone, 7330	[signature]	3/23	
Division Head Ruth H. Preller, 7300	[signature]	3/23	1. Release of this paper is approved. 2. To the best knowledge of this Division, the subject matter of this paper (has ____) (has never X) been classified.
Security, Code 1226	[signature]	4/6/09	1. Paper or abstract was released. 2. A copy is filed in this office. 35C 99-9
Office of Counsel, Code 1008.3	[signature]	4/7/09	
ADOR/Director NCST E. R. Franchi, 7000			
Public Affairs (Unclassified/ Unlimited Only), Code 7030.4	Carolyn L Gilioz	4/10/09	
Division, Code			
Author, Code			

HQ-NRL 5511/6 (Rev. 12-98) (e) THIS FORM CANCELS AND SUPERSEDES ALL PREVIOUS VERSIONS

APR 1 PM 5:22

Polarization characteristics of coastal waters and their impact on in-water visibility

Jing Zhou[1], Alberto Tonizzo[1], Alex Gilerson[1*], Michael Twardowski[2], Deric Gray[3], Alan Weidemann[3], Robert Arnone[3], Barry Gross[1], Fred Moshary[1], Sam Ahmed[1]
[1]Optical Remote Sensing Laboratory, the City College and the Graduate Center of CUNY, New York, NY, 10031, United States
[2]Department of Research, WET Labs, Inc., 165 Dean Knauss Dr., Narragansett, Rhode Island, 02882, United States
[3]Naval Research Laboratory, Code 7333, Stennis Space Center, Mississippi, 39529, United States

ABSTRACT

Polarization characteristics of coastal waters were recently measured during a cruise on the R/V "Connecticut" in the areas of New York Harbor - Sandy Hook, NJ region using a new Stokes vector instrument developed by the Optical Remote Sensing Laboratory at CCNY. The instrument has three hyperspectral Satlantic radiance sensors each with a polarizer positioned in front of it, with polarization axes aligned at 0, 90 and 45°. The measured degrees of polarization (DOPs) and normalized radiances as a function of angle and wavelength match very well with simulated ones obtained with a Monte Carlo radiative transfer code for the atmosphere-ocean system. In order to numerically reproduce the polarized images for underwater horizontal imaging system the measured typical underwater polarized radiance was used to estimate the polarized components of the background veiling light and the blurring effects were modeled by point spread functions obtained from the measured volume scattering functions from this cruise and other typical oceanic environments. It is shown that the visibility can be improved for unpolarized target by placing a polarizer oriented orthogonally to the partially polarized direction of the veiling light before camera. The blurring effects strongly depend on the small angle scattering in the forward directions. For polarized targets the Monte Carlo simulation of slab geometry for polarized pencil light shows that the seattering medium with high *g* value has a very strong ability to retain the polarization status of the incident light, which can be utilized to improve the image contrasts for targets with very different polarized reflection properties.

Keywords: Polarization, volume scattering function, visibility.

1. INTRODUCTION

Study of the underwater polarized light field can lead to significant improvements of underwater visibility. Polarization-sensitive vision is well documented as serving in navigation and enhancement of target detection for many marine species [1]. Knowledge of the underwater polarization pattern can help us better understand the mechanisms involved in the sensitivity of animals to the polarization of light and the manners in which these animals utilize underwater polarization. Inspired by biological visual systems, many studies have applied various polarization techniques in underwater imaging systems to improve the visibility of selected target features in a scattering medium [2-5]. Since the underwater scattered light, or *veiling light*, is the dominant cause of image degradation, assessing the effectiveness of these polarization techniques under natural illumination also relies on the analysis of the spectral and geometrical angular dependence of the underwater polarized light field. When compared with standard radiance intensity data, the polarized upwelling radiance is more sensitive to the intrinsic nature of in-water particulates such as particle size, shape and refractive index [6, 7]; therefore it carries more information on the background veiling light.

Despite the importance of the underwater polarization for marine applications most of the previous studies were based on theoretical calculations due to the lack of appropriate instrumentation to perform accurate and reliable polarization measurements [6, 8]. Recently we developed a hyperspectral and multiangular polarimeter capable of performing *in-situ*

* gilerson@ccny.cuny.edu

Ocean Sensing and Monitoring, edited by Weilin (Will) Hou, Proc. of SPIE Vol. 7317, 73170H
© 2009 SPIE · CCC code: 0277-786X/09/$18 · doi: 10.1117/12.820738

measurements of the underwater polarized radiance [9]. In this paper, typical patterns of the underwater polarization obtained with this instrument during a cruise in the coastal areas of New York Harbor - Sandy Hook, NJ region will be presented, after a brief description of the instrumentation. The correctness of the experimental data was confirmed by the results of the Monte Carlo radiative transfer simulations for the atmosphere-ocean system. In order to determine the effects of a scattering medium on the quality of underwater imaging, the point-spread function, obtained from the measured VSF, and the measured polarized pattern are combined to numerically reproduce the image of a standard Air Force Target under natural illumination conditions. Results obtained by using different VSFs measured in various oceanic environments were then compared, focusing on the impact on underwater visibility.

2. UNDERWATER POLARIZATION MEASUREMENTS

2.1 The polarimeter and the cruise

The polarimeter consists of three Satlantic Hyperspectral radiance sensors with a polarizer attached in front of each one. The orientations of the polarizers are: 0° (vertical), 90° (horizontal) and 45°. A stepper motor was used to rotate the sensors to cover the full 0-180° range of scattering angles, at 5° steps. A customized Labview program is responsible for the synchronization of the motor rotation and the data stream from the hyperspectral sensors and for the displaying the polarized spectra in real-time. If L_0, L_{90} and L_{45} are the radiances recorded by the three Satlantic sensors, then the DOP is given by:

$$DOP = \frac{\sqrt{(L_0 - L_{90})^2 + (2L_{45} - L_{90} - L_0)^2}}{L} \qquad (1)$$

where $L = L_0 + L_{90}$ is the total intensity. For normalization purposes, the downwelling irradiance, E_d was also monitored with a Satlantic Hyperspectral irradiance sensor positioned on deck of the boat. Water optical properties were measured by an AC-9 instrument (WET Labs, Inc.). VSF measurements were obtained with a custom device called the MASCOT, which uses a 658 nm laser diode source and 17 independent detectors to measure the VSF from 10 to 170° in 10° increments. Data were collected at 8 stations during a recent cruise on the R/V "Connecticut" in the coastal areas of New York Harbor - Sandy Hook, NJ region, on July 21-23 2008.

2.2 Typical angular DOP distribution

From in-water optical measurements at all stations, chlorophyll concentrations were estimated to be in the range 1.3-4.8μg/l, minerals concentrations 2.0-3.9mg/l, and CDOM absorption at 400 nm approximately 0.5 m^{-1}. Fig. 1 shows the typical angular distributions of the normalized radiance (Fig. 1a) and the DOP (Fig. 1b) at 510nm for measurements 1m below the water surface. Generally speaking, the DOP presents a bell-shaped angular distribution with maximal values around 100° and minima in proximity of 0 and 180°. The highest value of the DOP is approximately 0.4 during sunny days, which is lower than half the value predicted by Rayleigh theory. This value can be even lower during cloudy days. Interested readers can find more detailed descriptions of the instruments and data in [9].

Figure 1 also shows the simulated radiance and DOP vs. scattering angle obtained with a Monte Carlo method using the measured IOP and VSF values. As it can be seen, simulations and experimental results match quite well. Figure 2 shows the comparison between MASCOT and Petzold's phase function, for Station 1. Similar results were obtained for Stations 4, 5 and 7, due to similar water compositions.

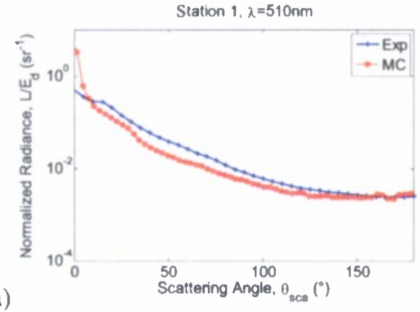

(a)

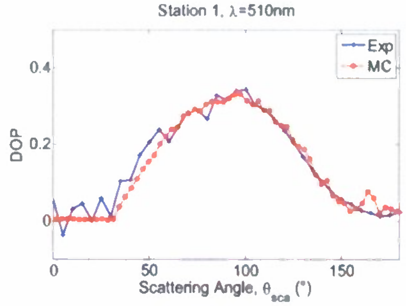

(b)

Fig. 1. a) Angular radiance normalized to downwelling irradiance. b) DOP angular distribution at λ=510nm.

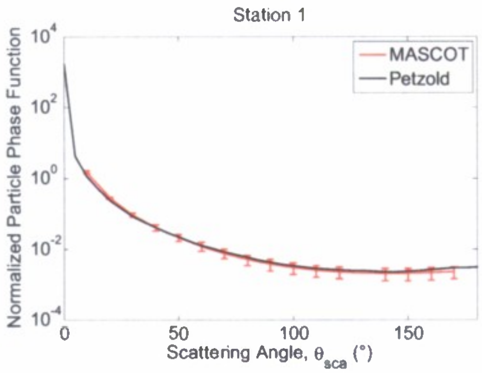

Fig. 2. Comparison of MASCOT measurements and standard Petzold functions.

3. UNDERWATER VISIBILITY ASSESSMENT FOR UNPOLARIZED TARGETS

3.1 Image modeling

Under natural illumination an imaging system measures light from the target and additional light (veiling light) from the intervening medium In addition, light from the target experiences scattering when it passes through the scattering medium between the target and the camera, hence the image gets blurred. This blurring effect can be fully described by the PSF of the scattering medium [10]. In this section an image model will be first introduced to combine together blurring and veiling light in order to simulate the imaging quality in the water scattering medium for an unpolarized target. Then the underwater visibility will be assessed and discussed by applying various particulate phase functions as well as various polarization techniques.

Let's consider an underwater object illuminated by sun light and a camera taking pictures looking horizontally (as shown in Fig. 3). On the image plane, the irradiance signal from the target S is given by the convolution of its reflection map $r(x,y)$ and the PSF of the water medium $p(x,y)$, *i.e.*:

$$S = r(x,y) \otimes p(x,y) \tag{2}$$

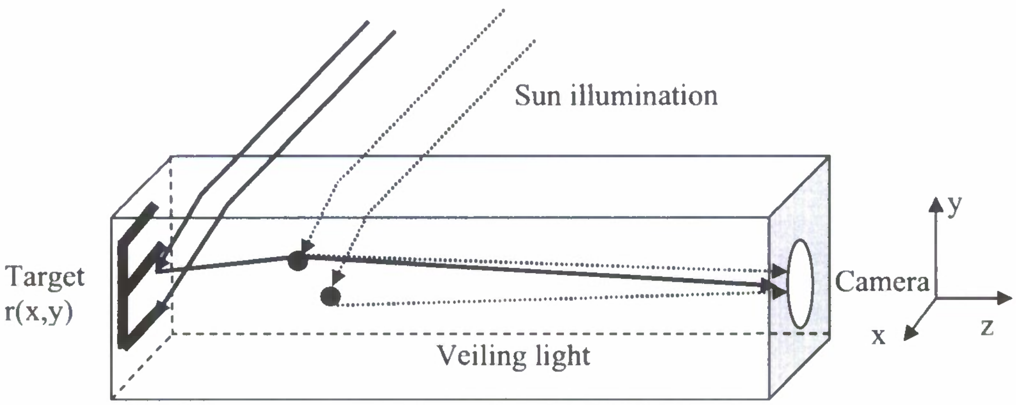

Fig. 3 Diagram of imaging geometry for image modeling

Note here that the target is assumed to completely depolarize the incident light and diffusely reflect the sun light acting like a lambertian surface. The scattered light from each layer dz between the target and the camera reaches the camera experiencing an attenuation equal to $exp(-cz)$. The total veiling light is then obtained integrating over all the layers between 0 and Z (the distance between the target and the camera). Therefore approximated veiling light irradiance should have the following form, assuming that single scattering is dominant:

$$V(Z) = V(\theta,\infty)(1-\exp(-cZ)) \tag{3}$$

The term $V(\theta,\infty)$ is the background light without the target or with the target extended to infinity, which can be estimated from our angular underwater radiance measurement:

$$V(\theta,\infty) = 2\pi \int_{\theta_{min}}^{\theta_{max}} L(\theta)\sin\theta d\theta \tag{4}$$

θ_{min} and θ_{max} are, respectively, the minimum and maximum angle of the particulate scattering extended to the camera aperture. Assuming that the scattered light keeps its polarization when passing through the medium, the linear polarized component of $V_{0/90}(\theta,\infty)$ has a form similar to (4), if $L(\theta)$ is replaced by its corresponding measured linear polarized components for 0 and 90°, which correspond to horizontal and vertical polarization:

$$V_{0/90}(\theta,\infty) = 2\pi \int_{\theta_{min}}^{\theta_{max}} L_{0/90}(\theta)\sin\theta d\theta \tag{5}$$

Then total signal collected by the camera is the sum of the blurred image and the veiling light, $E_T = S+V$.

3.2 Results

A Monte Carlo simulation is performed by using the measured phase function $\beta(\theta)$ to obtain the PSF at optical depth τ = 5 and single scattering albedo ω = 0.9. In addition to the measured $\beta(\theta)$ from our cruise, which resembles the standard Petzold function (shown in Fig. 2), $\beta(\theta)$ values obtained from other typical ocean environments were also used for comparison purposes. Specifically, $\beta(\theta)$ values were collected in Monterey Bay, in waters with mostly biological particulates, in Puget Sound with mostly sediment particles and in the Hudson Plume which belongs to oceanic environments [11]. The phase functions and corresponding PSFs were plotted in Fig. 4 together with the Petzold functions. The asymmetry factors g, defined as the cosine value weighted by phase function, are also calculated:

$$g = \int_{d\Omega} \cos(\theta)\beta(\theta)d\Omega \tag{6}$$

The g values for Petzold, biological, oceanic and sediment cases are 0.91, 0.97, 0.96, and 0.94 respectively. Although the four types of phase functions have a very close g values (above 0.9) oceanic case is the least peaked in the near forward direction. They are angularly flat in the backward direction but with different backscattering levels because of the different refractive indices of the dominant particulates. For example, the low refractive index of the biological particles leads to the lowest level of backscattering. Typical polarized angular radiances (corresponding to the angles at which the DOP reaches its maximal value) obtained from field measurements at 510nm were used in eq. (5) to estimate the veiling light background.

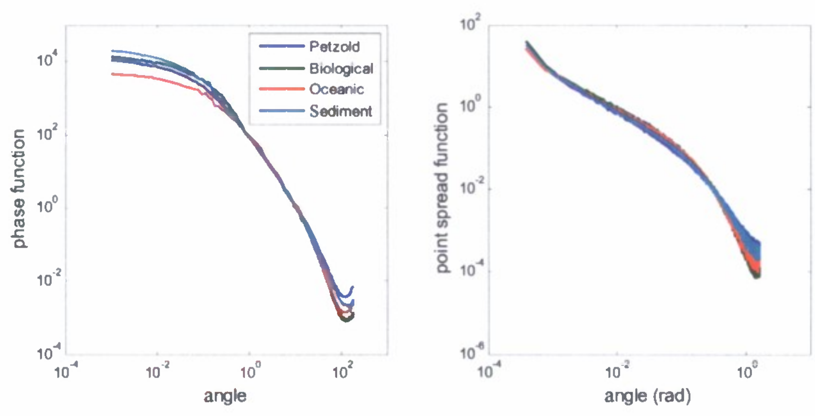

Fig. 4. a) Phase functions and b) PSFs (τ = 5 and ω = 0.9) for four types of typical ocean waters.

Whcn acquiring images of an unpolarized target looking in the horizontal direction (undcr sun illumination), a polarizer can be placed in front of the camera to rcmove all or part of the veiling light depending on thc DOP of the vciling light itself. This is due to the fact that, in this geometry, the scattered light at an angle corresponding to the horizontal direction (around 100° scattering angle) is partially linearly polarized, as it was shown in previous section. Fig. 5 displays thc results of the modeled image for the four types of phase functions shown in Fig. 4, thc target has a maximum reflection equal to 5%.

The blurred images under oceanic environment shows thc worst contrast among the four types of water conditions. This is related to the fact that its phasc function is the least forward peakcd among thcsc four environments. Thc vertically polarized images always show a better contrast than the intensity and the horizontally polarized ones. The images of the DOP are negatives of the intensity images because the morc unpolarizcd light from object rcpresents lower total DOP. Of course the effectiveness of image improvement increases with higher DOP of the veiling light.

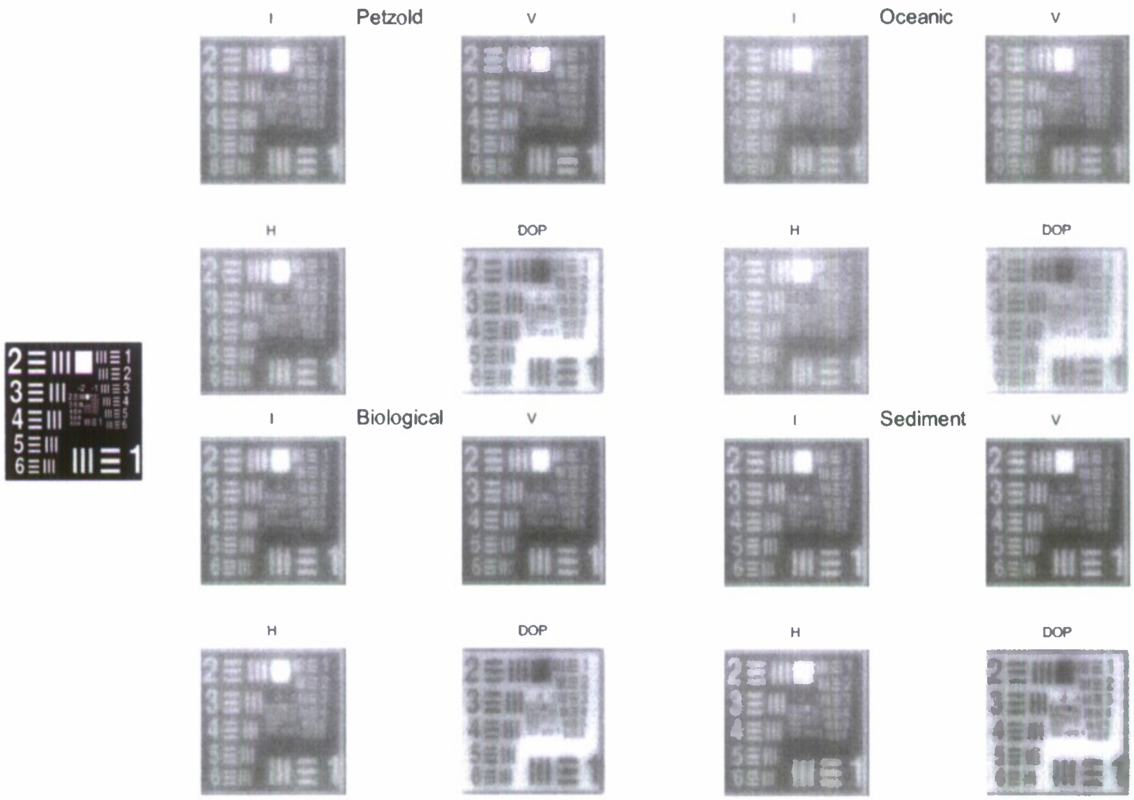

Fig. 5. Image modeling results of a standard Air Force Target using four types of phase functions with $\tau = 5$ and $\omega = 0.9$).

4. POLARIZED LIGHT TRAVELLING THROUGH A SCATTERING MEDIUM

The utilization of polarized techniques to enhance underwater detection rcquires that the polarizcd light producd by illumination sources or interactions such as scattering, surface reflection and transmission keep its polarization when it travels through a scattering medium. The visibility improvement based on polarization is determined by how far thc polarization information can bc carricd through thc scattering medium. In ordcr to cxaminc how linear polarizcd light spreads and depolarizes when travelling through the scattering mcdium, a Monte Carlo simulation based on slab geometry (Fig. 6) is performed. The polarized light is incident along the z axis and the detector array is placed in thc xy planc. Thc Stokes vector referring to the xz plane was calculated for each array element.

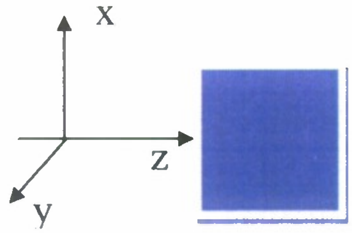

Fig.6 Slab geometry.

The phase function is obtained based on Mie theory with Junge size distribution $f(r) = r^{-\gamma}$ and refractive index 1.15 (relative to water). The following three cases were considered:

$$(1) r_{\min} = 0.1\mu m, r_{\max} = 10\mu m, \gamma = 3, g = 0.92$$
$$(2) r_{\min} = 0.1\mu m, r_{\max} = 10\mu m, \gamma = 5, g = 0.82$$
$$(3) r_{\min} = 0.01\mu m, r_{\max} = 10\mu m, \gamma = 5, g = 0.71$$

The DOP of the transmitted light is plotted in Fig. 7 with increasing optical depth for horizontally polarized incident light for the above three cases. The depolarization rate depends heavily on the g factor of the phase function [12]. The smaller the g factor is, the faster the DOP decreases with the optical depth. It is shown that the forward scattering has a very strong ability to retain its original polarization status even for optical depth higher than 10 when multiple scattering is dominant. Taking a typical g value of 0.91 for example, DOP is over 90% after a polarized light travelling through 10 optical depths. This can be used to distinguish objects with very different polarization reflectance properties.

The polarized images recorded keeping the same polarization as the incident light spread to larger angles with increasing optical depths as shown in Fig. 8. Its circularly symmetrical pattern resembles that of unpolarized incident light, implying limited resolution improvement by using polarized light illumination.

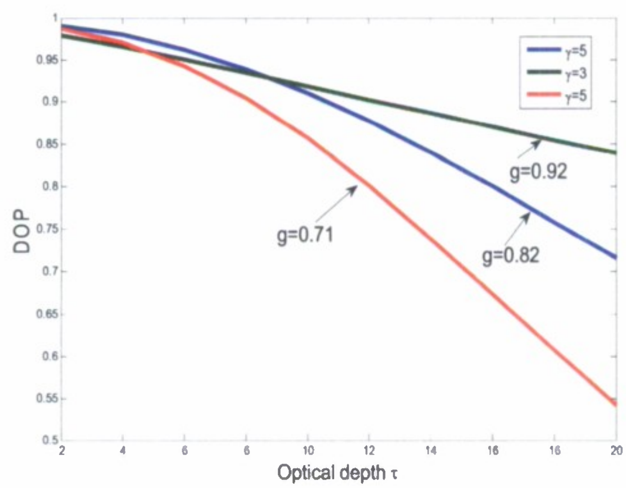

Fig.7. DOP as a function of optical depth for three g values

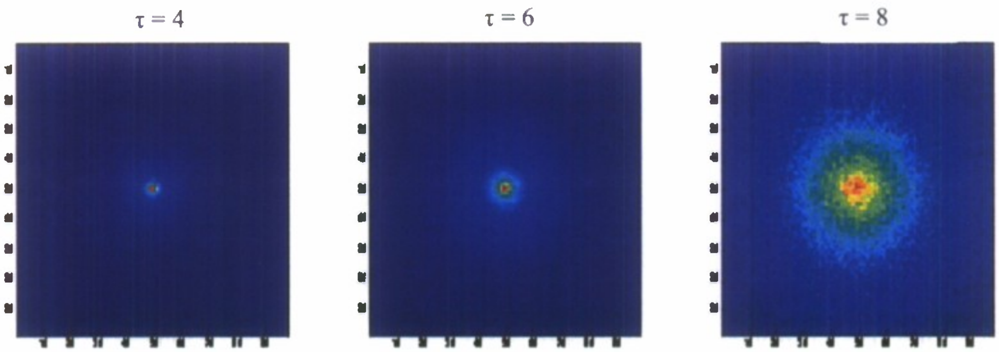

Fig.8. The spreading images of the horizontal polarized incident light along z axis with the polarizer oriented horizontally before the detector array

5. SUMMARY AND CONCLUSIONS

Underwater polarization characteristics were measured in the coastal areas of New York Harbor - Sandy Hook using a new hyperspectral multiangular polarimeter recently developed by the Optical Remote Sensing Laboratory at CCNY. The angular distribution of DOP always exhibits a bell shape with a maximal value of 0.4 around 100° scattering angle for the examined waters which have chlorophyll concentrations 1.3-4.8μg/l, minerals concentrations 12.0-3.9mg/l, and CDOM absorption at 400 nm approximately 0.5 m^{-1}. These experimental results are also confirmed with vector radiative transfer simulations based on Monte Carlo methods.

The measured polarized radiance and volume scattering data were utilized to model the underwater images of unpolarized targets. The veiling light level is estimated from the measured polarized radiance and the PSF is obtained through a Monte Carlo method using the measured VSF. Taking advantage of the targets' lack of polarization and partially horizontal polarization of the background radiance, the veiling light can be reduced by placing a vertically oriented polarizer before the imaging system and thus improving the visibility. Four types of VSFs under typical ocean environments were applied to model the blurred images. At the same optical depth the quality of the underwater images strongly depends on the small angle scattering. The ocean condition with the least peaked forward scattering, the oceanic case, has the worst image quality.

On the other hand, the Monte Carlo simulation of slab geometry for polarized pencil light shows that the scattering medium with high g value has a very strong ability to retain the polarization status of the incident light, which can be utilized to improve the image contrasts for targets with very different polarized reflection properties. Evaluations of imaging the polarized targets by using polarization techniques should be the next steps of research.

ACKNOWLEDGEMENTS

This research has been supported by grants from the Office of Naval Research, NASA and NOAA.

REFERENCES

[1] Shai Sabbah, Amit lerner, Carynelisa Erlick and Nadav Shashar, "Under water polarization vision – A physical examination", Recent Res. Devel. Experimental& Theoretical Bio., 1 (2005).
[2] J. S. Tyo, M. P. Rowe, E. N. Pugh, Jr., and N. Engheta, ''Target detection in optically scattering media by polarization-difference imaging,'' Appl. Opt. 35, 1855–1870 (1996).
[3] George W. Kattawar and Milun J. Rakovic, "Virtues of Muller matrix imaging for underwater target detection", Appl. Opt. 38, No. 30, 6431-6438 (1999).
[4] Yoav Y. Schechner and Nir Karpel, "Clear Underwater Vision", Proc. Computer Vision & pattern recognition, I, 536-543 (2004).

[5] Peter C. Y. Chang, Jonathan C. Flitton, Keith I. Hopcraft, Eric Jakeman, David L. Jordan, and John G. Walker, "Improving visibility depth in passive underwater imaging by use of polarization", Appl. Opt. 42, No. 15, 2794-2803 (2003).
[6] M. Chami, R. Santer, E. Dilligeard, "Radiative transfer model for the computation of radiance and polarization in an ocean-atmosphere system: polarization properties of suspended matter for remote sensing," Appl. Opt. 40, 2938-2416 (2001).
[7] M. Chami and D. McKee, "Determination of biogeochemical properties of marine particles using above water measurements of the degree of polarization at the Brewster angle," Opt. Exp. 15, 9494-9509 (2007).
[8] J. Chowdhary, B. Cairns, L. D. Travis, "Contribution of water-leaving radiances to multiangle, multispectral polarimetric observations over the open ocean: bio-optical model results for case 1 waters," Appl. Opt. 45, 5542-5567 (2006).
[9] A. Tonizzo, J. Zhou, A. Gilerson, M. Twardowski, D. Gray, R. Arnone, B. Gross, F. Moshary and S. Ahmed, "Polarized light in coastal waters: hyperspectral and multiangular analysis", Opt. Exp., accepted. (2009).
[10] Weilin Hou, Deric J Gray, Alan D. Weidemann and Robert A Arnone, "Comparison and validation of point spread models for imaging in natural waters", Opt. Exp. 16, No. 13, 9958-9965 (2008).
[11] Gray, Deric J, Weidemann, Alan D, "Volume scattering function effects on underwater imaging systems", poster session, Ocean Optics XX (2008).
[12] Jessica C. Ramella-Roman, Scott A. Prahl, Steven L. Jacques, "Three Monte Carlo programs of polarized light transport into scattering media: Part II", Opt. Exp. 13, No. 25, 10392-10405 (2005).